Electronic Supplementary Information

One-pot synthesized anthracene-based chemodosimeter for toxic cyanide (CN^-) detection and anticancer analysis: Substantiated by DFT, real-time investigations, and cytotoxicity assays

Muthaiah Shellaiah[a], Wen-Tai Li[b, c*], Phamdom Romabai Chanu[d], Richard Lam[b], Arumugam Murugan[e], Basheer Aazaad[f], Ming-Chang Lin[g, h], K. Anandan[i], and Mayank Bhushan[j]

[a]Department of Chemistry, Dayananda Sagar College of Engineering, Bangalore, Karnataka, India-560111.

[b]National Research Institute of Chinese Medicine, Ministry of Health and Welfare, Taipei 11221, Taiwan, ROC.

[c]Department of Chemistry, Tamkang University, New Taipei City 251301, Taiwan, ROC

[d]College of Pharmacy, Taipei Medical University 11031, Taiwan, ROC.

[e]Department of Chemistry, North Eastern Regional Institute of Science & Technology, Nirjuli, Itanagar 791109, India

[f]Department of Physics, Saveetha Engineering College, Thandalam, Chennai – 602105, Tamilnadu, India.

[g]Department of Applied Chemistry, National Yang Ming Chiao Tung University, Hsinchu 300, Taiwan.

[h]Center for Emergent Functional Matter Science, National Yang Ming Chiao Tung University, Hsinchu 300, Taiwan

[i]Department of Physics, AMET University, Chennai 603 112, Tamil Nadu, India

[j]Department of Biotechnology, Graphic Era (Deemed to be University), Dehradun 248002, Uttarakhand, India

*Email: wtli@nricm.edu.tw

Table of contents

General Information

The purity of AN and their peak variations in the presence of CN^- ions were elucidated by ^1H and ^{13}C NMR spectral data obtained on a Bruker 600 MHz spectrometer (^1H: 600 MHz; ^{13}C: 151 MHz), using deuterated dimethyl sulfoxide (D_6-DMSO) as the solvent. Chemical shifts (δ) and coupling constants (J) were reported in ppm and Hz, respectively. Mass analysis was carried out on a Q Exactive Orbitrap MS mass spectrometer (Thermo Fisher Scientific, USA). UV-Visible spectroscopic investigations were performed using a SpectraMax M5 microplate reader (Molecular Devices, USA). Fourier Transform Infrared (FTIR) spectral analysis was carried out using a Thermo Scientific Nicolet iS50 FTIR spectrometer (Thermo Fisher Scientific, USA). The pH effect studies used freshly prepared pH 1–14 buffers.[1-3] The strip method was performed using Whatman filter paper. Cotton buds were purchased from a nearby supermarket. Fish was purchased from the Beitou market in Taipei City, Taiwan (ROC).

Stock Solutions[4]

Anions such as Cl^- (Chloride), Br^- (Bromide), I^- (Iodide), CN^- (Cyanide), F^- (Fluoride), ClO_4^- (Perchlorate), SO_4^{2-} (Sulfate), $S_2O_3^{2-}$ (Thiosulfate), PO_4^{3-} (Phosphate), HCO_3^- (Bicarbonate), NO_2^- (Nitrite), $H_2PO_4^-$ (Dihydrogen Phosphate), CO_3^{2-} (Carbonate), HSO_3^- (Bisulfite), N_3^- (Azide), CA (Cysteamine), Cys (Cysteine), Na_2S (Sodium Sulfide), and GSH (Glutathione) were prepared in DI water at 100 mM concentration.

Procedure for pH effect studies[5]

pH effect studies were carried out by following combinations: (A) 50 µL of AN (from 1 mM stock) + 900 µL of DMSO + 50 µL of respective pH buffers (from 100 mM stock) and (B) 50 µL of AN (from 1 mM stock) + 895 µL of DMSO + 50 µL of respective pH buffers (from

100 mM stock) + 5 µL of CN^- ions (from 100 mM stock). The samples were shaken well and subjected to PL interrogations.

Relative photoluminescence quantum yield (PLQY) calculation[6]

To calculate the quantum yield of probe AN, the 9,10-diphenylanthracene (Φ_F = 70% in DMSO) was used as the reference using the following formula:

$$\Phi_{sample} = \Phi_{std}(I_{sample}/I_{std})(A_{std}/A_{sample})(\eta_{sample}/\eta_{std})^2,$$

where Φ_{std} stands for the quantum yield of the reference sample (9,10-diphenylanthracene), I_{sample}/I_{std} represents the intensity ratio of the sample (L) and standard (Fluorescein), A_{std}/A_{sample} is the absorbance ratio of sample and standard, and η_{sample}/η_{std} is the ratio of refractive indices.

NMR titration and HR-Mass data of AN + CN^-[4, 7]

10 mM of AN (1 equiv. in DMSO-d_6) was mixed with 5 mM (0.5 equiv.), 10 mM (1 equiv.), and 30 mM (3 equiv.) of TBACN DMSO-d_6 and then subjected to ^{1}H-NMR interrogations. The AN + CN^- (at 1 equiv.: 3 equiv.) mixture was subjected to ^{13}C-NMR spectral investigation to confirm the ANCN formation further. The data were plotted in a stacked plot. HR-Mass analysis was performed by injecting an AN + CN^- mixture at 1 equiv.:3 equiv. in DMSO solution (Note: 3 equiv. of CN^- ions was used to maintain a stable environment to form ANCN chemodosimetric product).

FTIR data of AN + CN^-[5]

In a vial, 10 mg of AN (1 equiv.) was stirred with 33 mg of TBACN (3 equiv.) in DMSO + ACN (1 mL + 1 mL) at 180°C for five days. After the complete evaporation of solvent, the vial was kept inside the oven at 60°C for two days. Then the dried solid sample was subjected to FTIR investigation along with AN and TBACN.

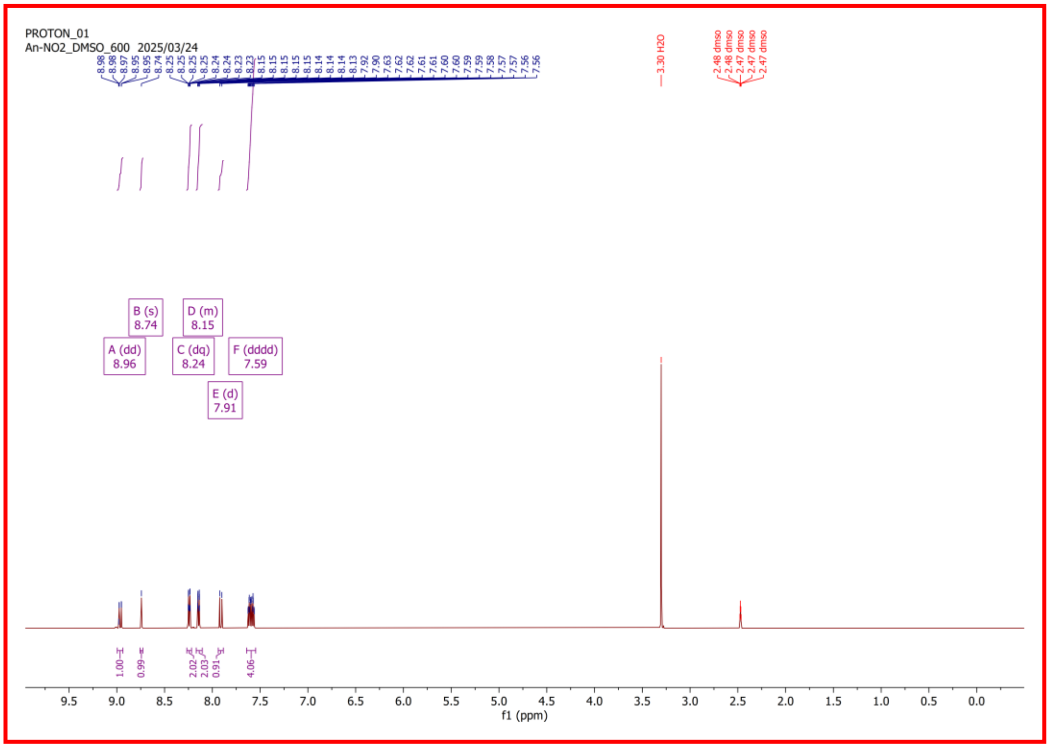

Figure S1. ^{1}H NMR spectra of AN.

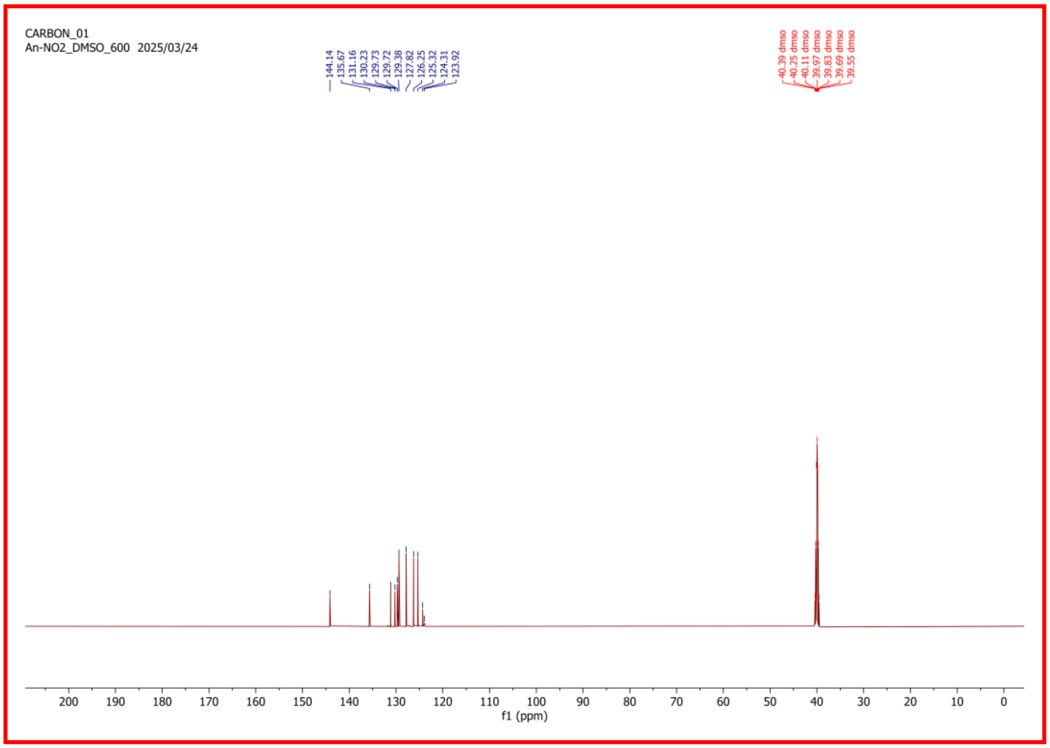

Figure S2. ^{13}C NMR spectra of AN.

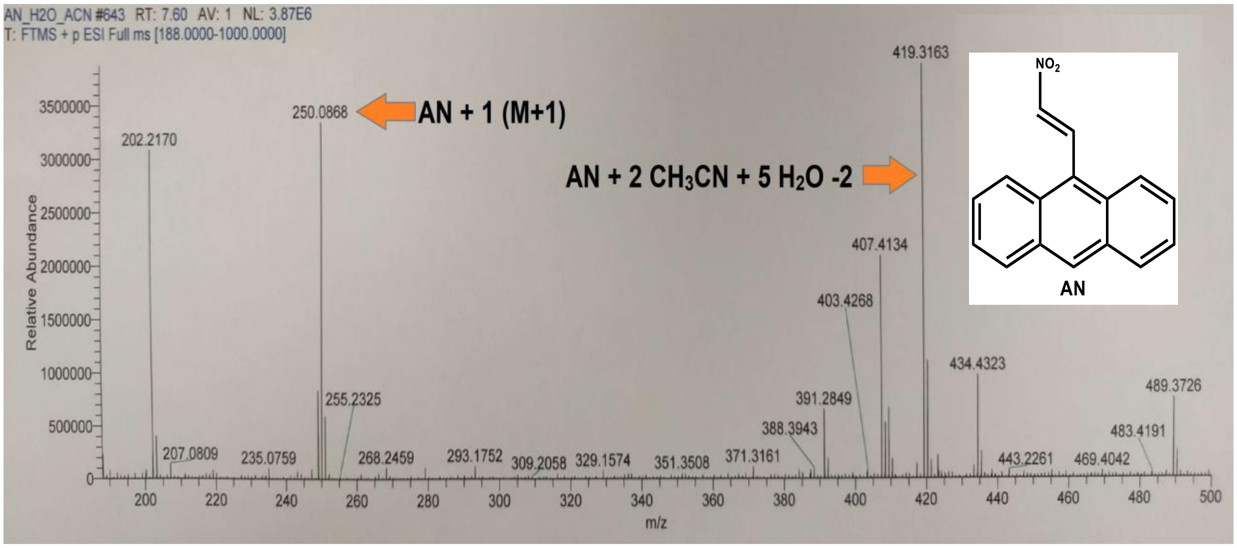

Figure S3. HR-Mass spectra of AN.

Table S1. Relative photoluminescence quantum yield (PLQY; Φ_F) values and fold of PL enhancement of AN (50 µM) in the presence of 500 µM of cyanide (CN^-) ions in diverse solvents.

Data	DMSO	DMF	EtOH	ACN	THF	Water
Φ_F of AN (%)	0.92	0.88	0.94	0.83	0.89	1.04
Φ_F of AN + CN^- (%)	18.73	17.34	6.65	11.56	9.54	3.78
I/I_0 of AN + CN^- at 420 nm	20.08	18.76	7.11	12.42	10.05	4.78

9,10-Diphenylanthracene in DMSO (Φ_F = 70%) was used as a reference standard for PLQY measurement.

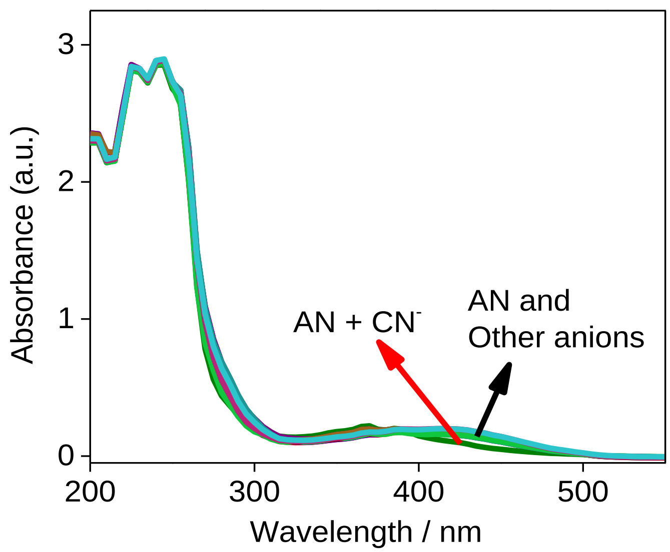

Figure S4. UV-Visible selectivity of AN towards anion (scan range = 200-550 nm).

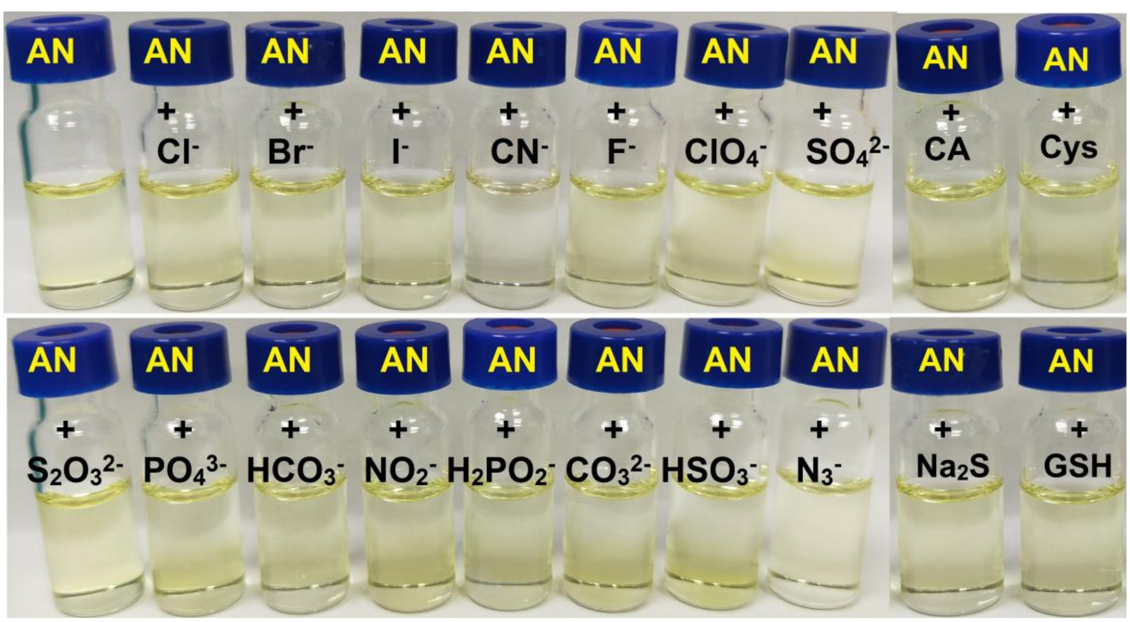

Figure S5. Colorimetric response of 50 µM of AN to 500 µM of anions in DMSO.

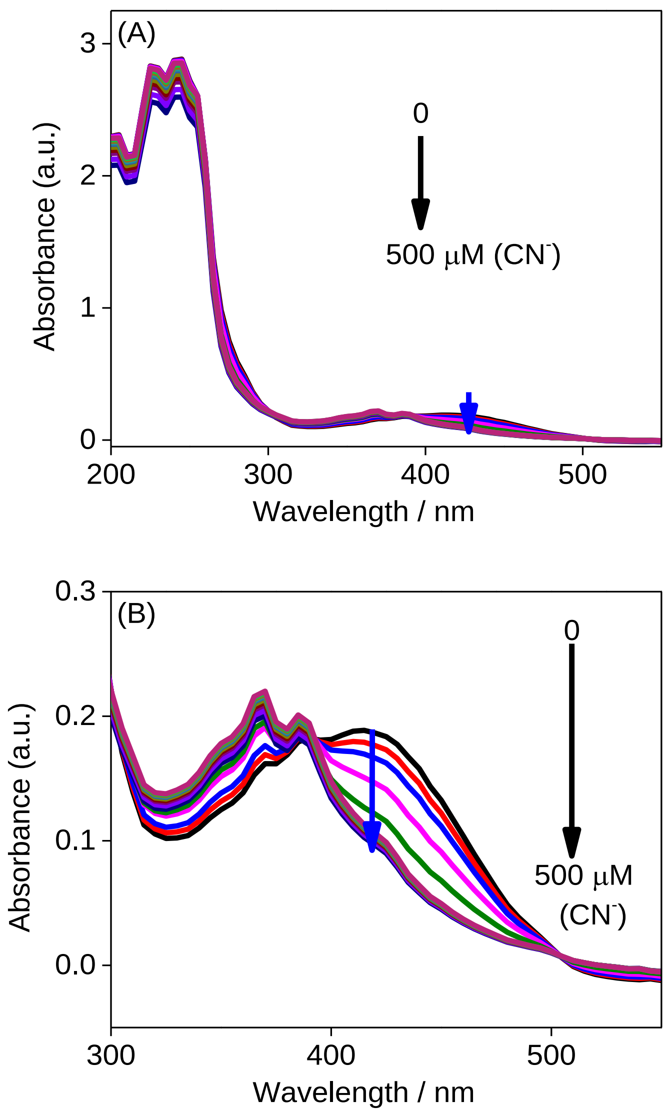

Figure S6. (A, B) UV-Visible titration of AN (50 μM) with 0-500 μM CN^- ions in DMSO.

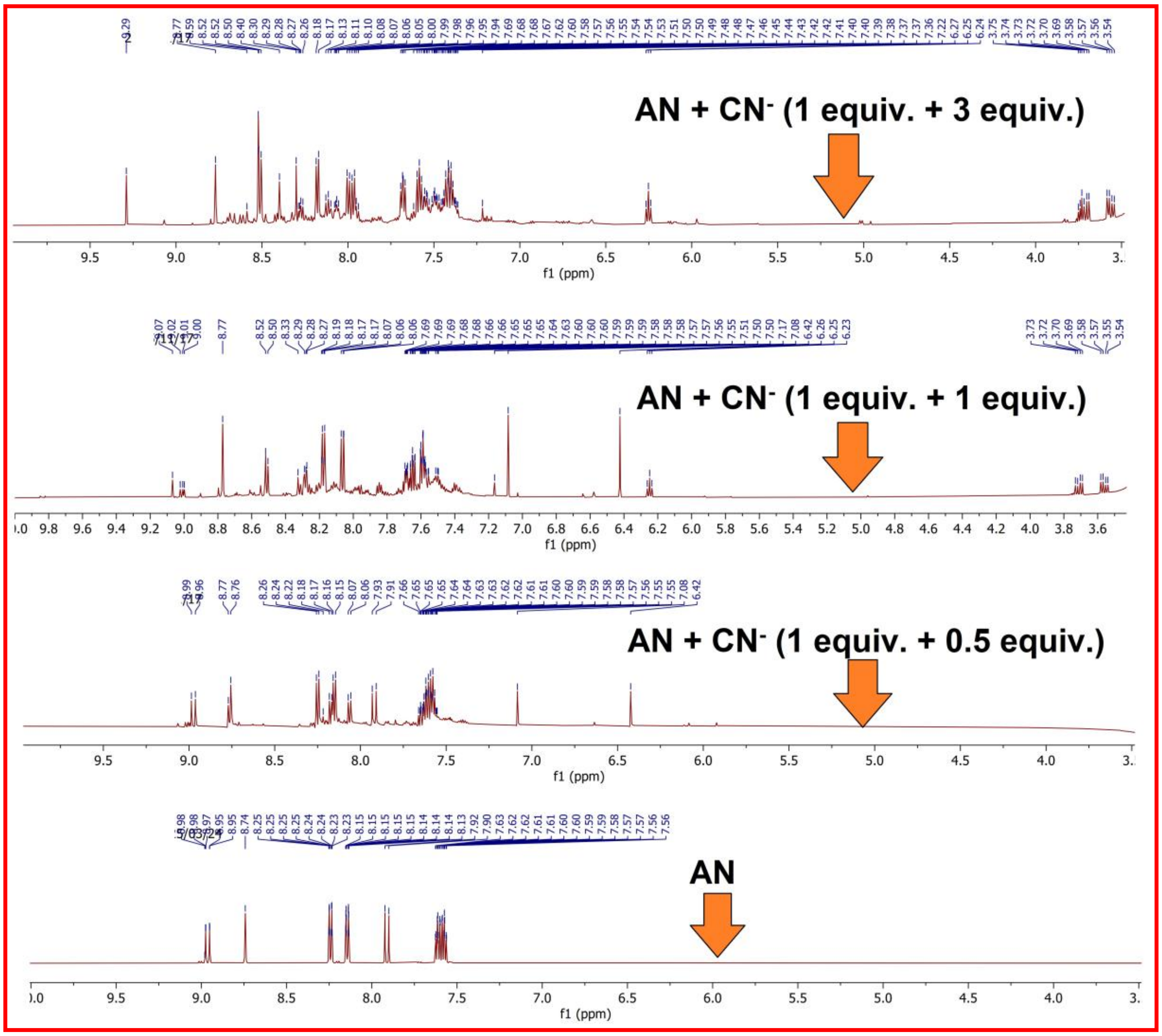

Figure S7. [1]H-NMR titration of AN (10 mM) with 5-30 mM of TBACN in DMSO-d_6.

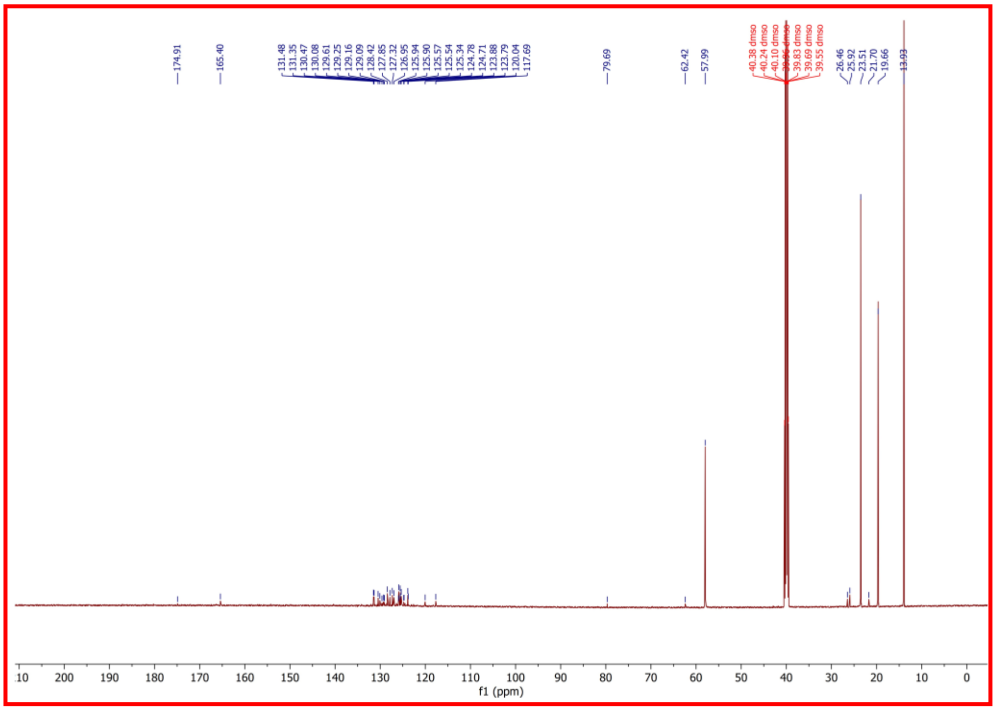

Figure S8. ^{13}C-NMR spectra of AN (10 mM; 1 equiv.) in the presence of CN^- (30 mM; 3 equiv.) confirm the ANCN formation.

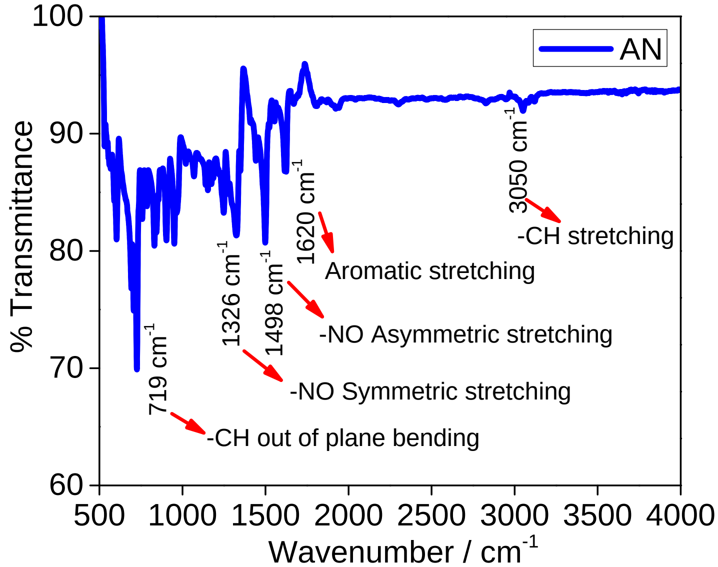

Figure S9. FTIR spectra of AN.

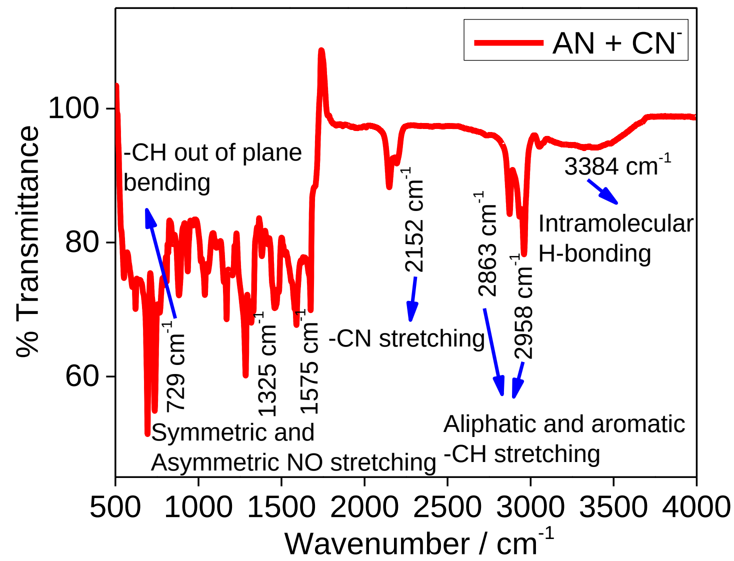

Figure S10. FTIR spectra of AN + CN^- ions.

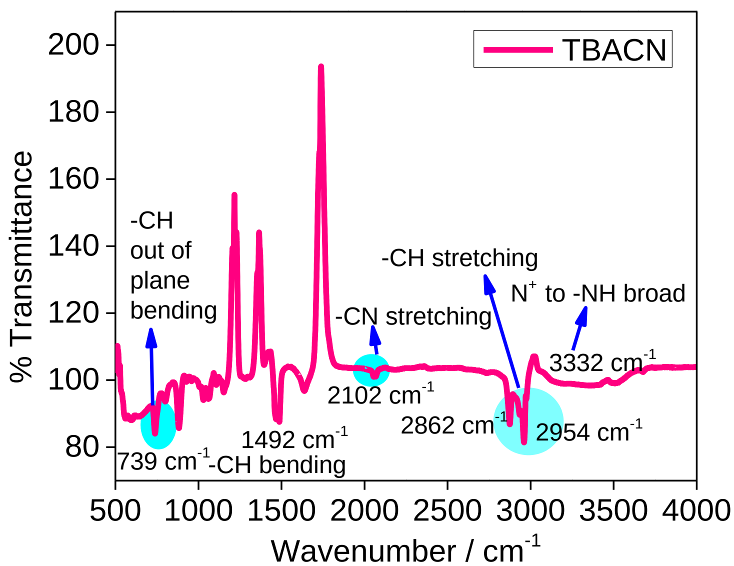

Figure S11. FTIR spectra of tetrabutylammonium cyanide (TBACN).

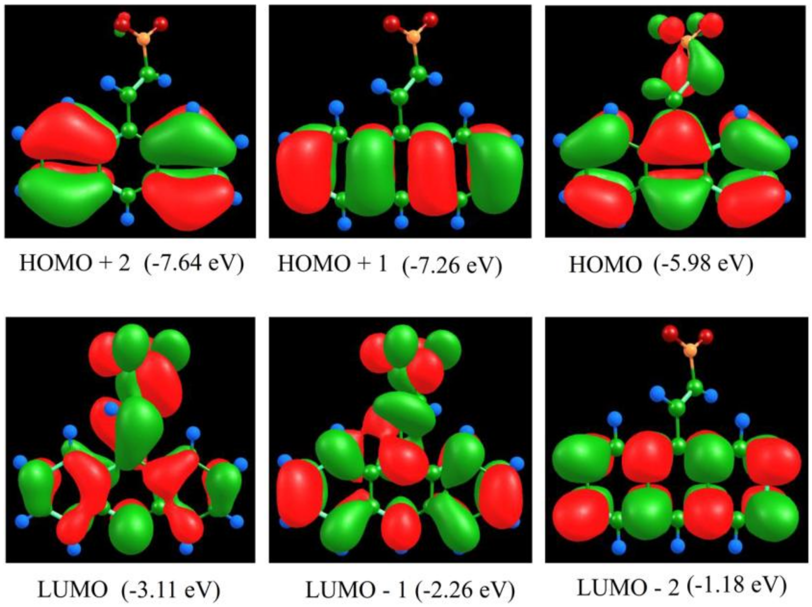

Figure S12. HOMOs and LUMOs of AN under gas phase optimized by B3LYP/6-31+G(d,p) level of theory/basis set.

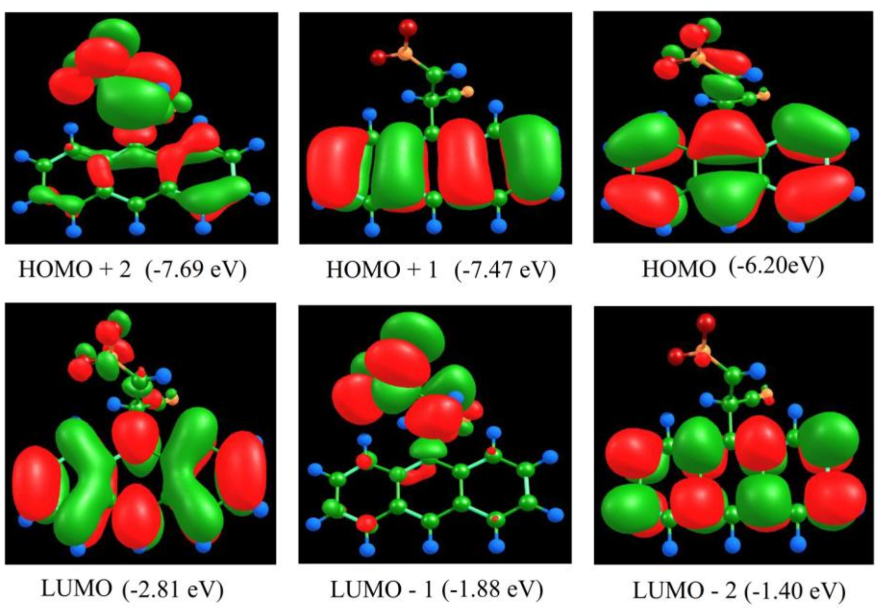

Figure S13. HOMOs and LUMOs of ANCN under gas phase optimized by B3LYP/6-31+G(d,p) level of theory/basis set.

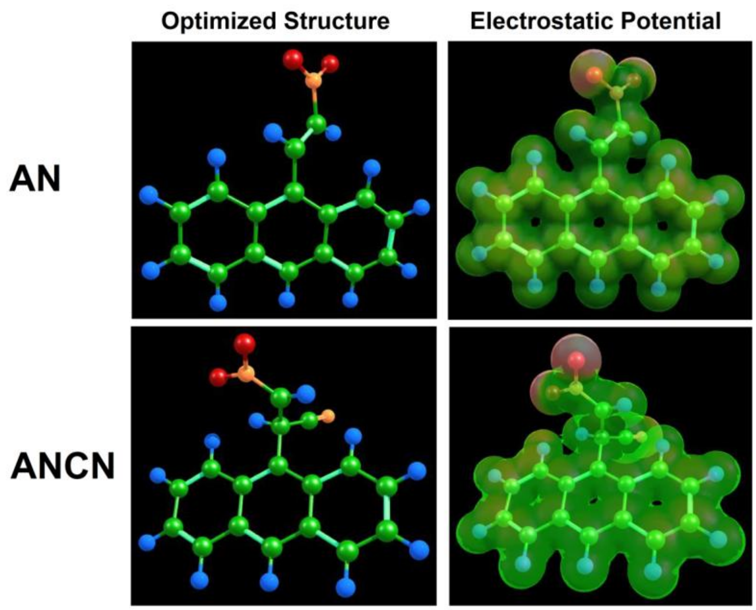

Figure S14. Optimized structure and Electrostatic Potential of AN and ANCN under solvent (DMSO) phase by B3LYP/6-31+G(d,p) level of theory/basis set.

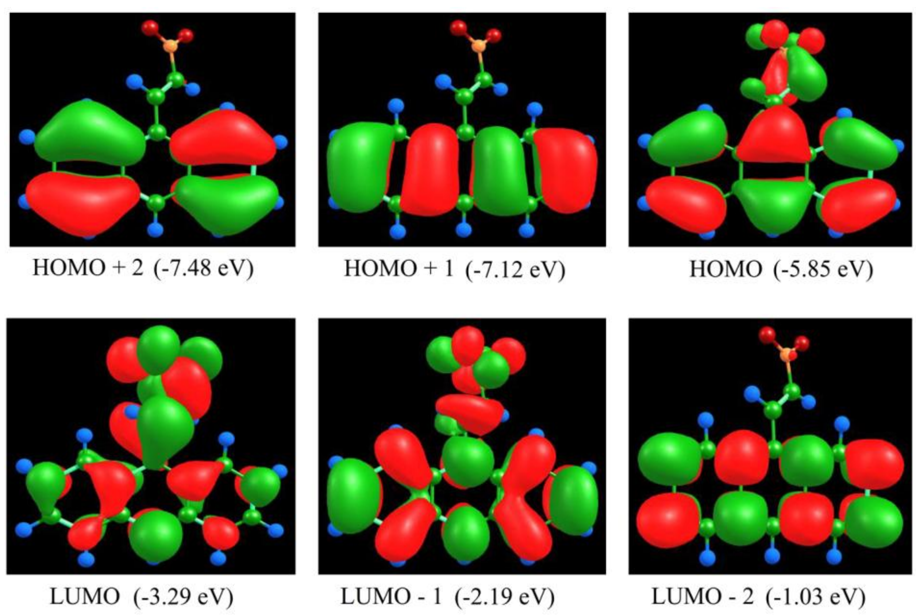

Figure S15. HOMOs and LUMOs of AN under solvent (DMSO) phase optimized by B3LYP/6-31+G(d,p) level of theory/basis set.

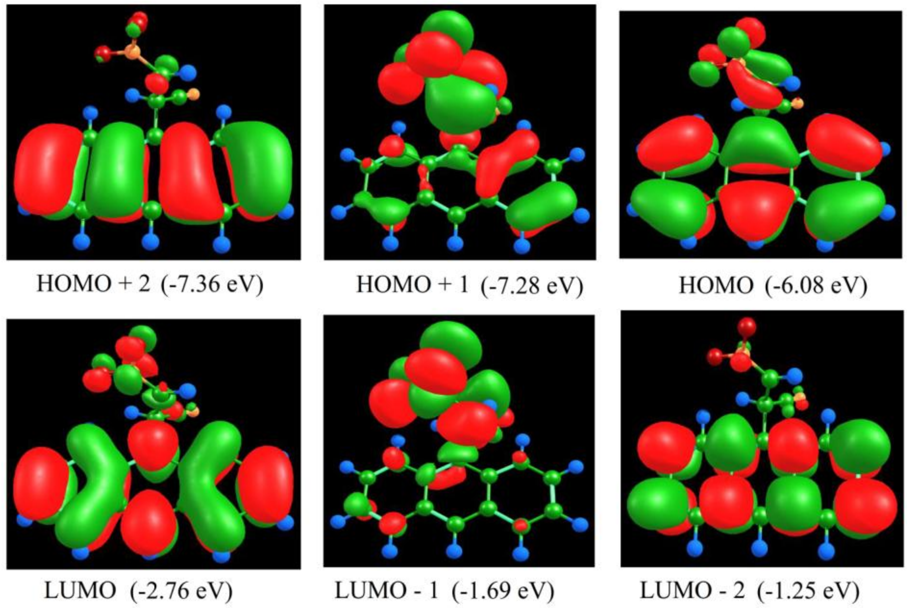

Figure S16. HOMOs and LUMOs of ANCN under solvent (DMSO) phase optimized by B3LYP/6-31+G(d,p) level of theory/basis set.

Table S2: HOMOs, LUMOs and band gaps of AN and ANCN optimized under gas and DMSO solvent phase by B3LYP/6-31+G(d,p).

Medium / Orbital	Gas (eV)		DMSO (eV)	
	AN	ANCN	AN	ANCN
HOMO + 2	-7.64	-7.69	-7.48	-7.36
HOMO + 1	-7.26	-7.47	-7.12	-7.28
HOMO	-5.98	-6.20	-5.85	-6.08
LUMO	-3.11	-2.81	-3.29	-2.76
LUMO – 1	-2.26	-1.88	-2.19	-1.69
LUMO – 2	-1.18	-1.40	-1.03	-1.25
H-L gap	2.87	3.39	2.56	3.32

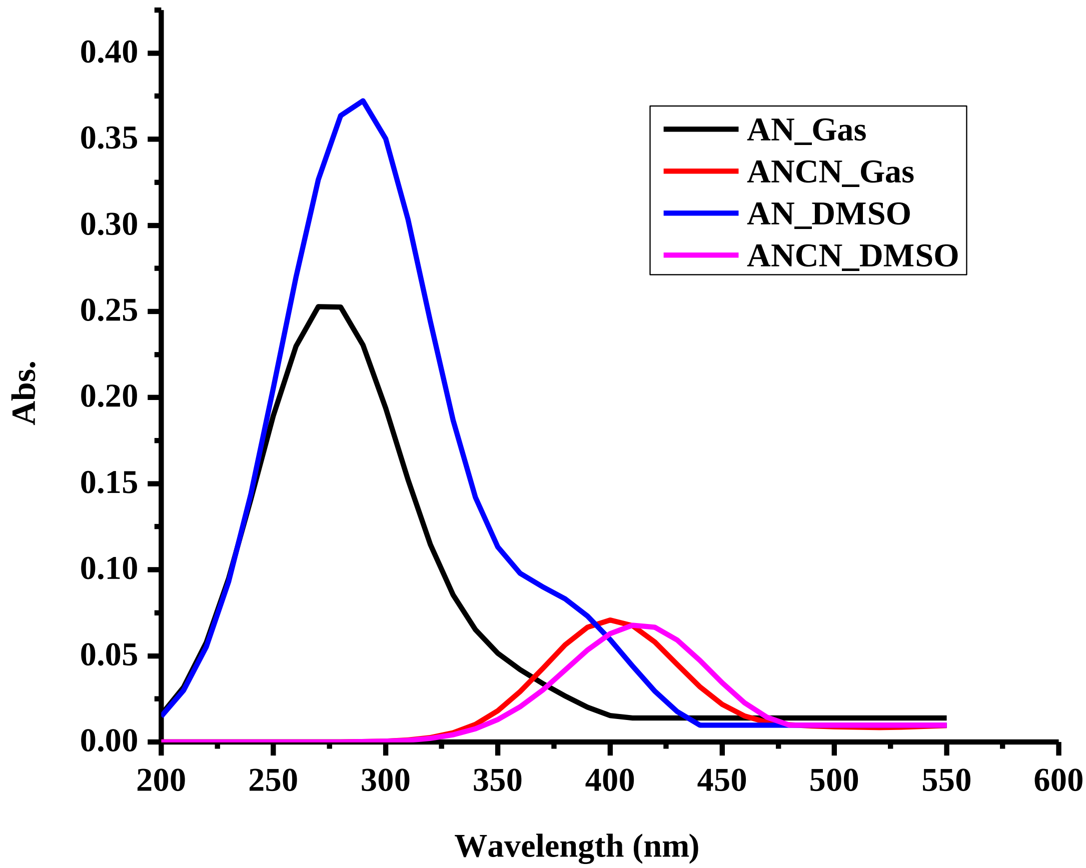

Figure S17. The simulated (TD-DFT) absorption spectra of AN and ANCN in gas and DMSO.

Table S3. TD-DFT results on absorption wavelength peaks.

	Gas	**DMSO**
AN	273 nm	289 nm and 296 nm
ANCN	400 nm	416 nm

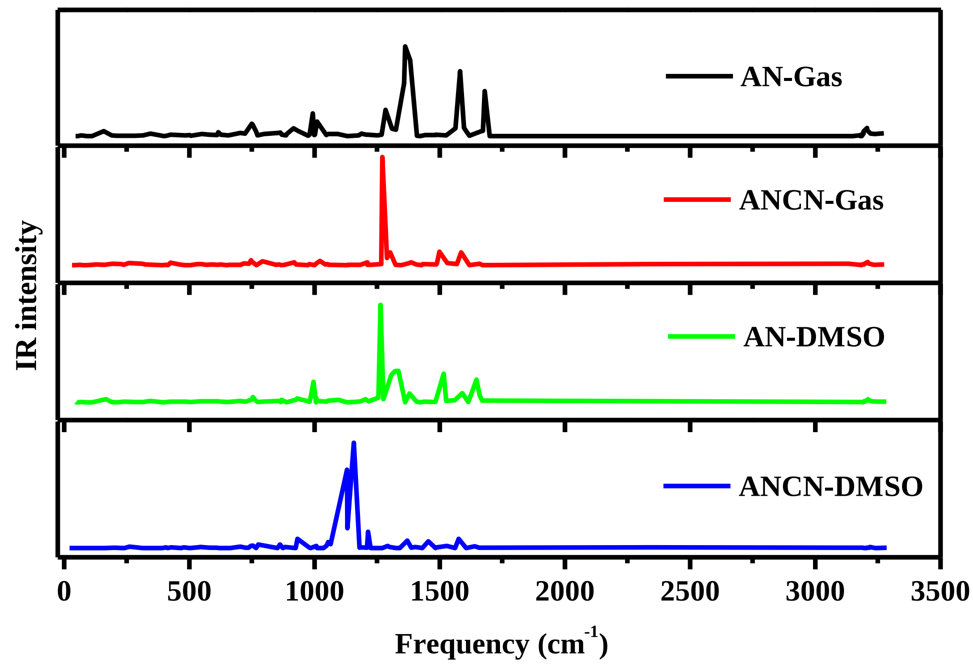

Figure S18. DFT optimized FTIR spectrum of AN and ANCN in gas and DMSO state.

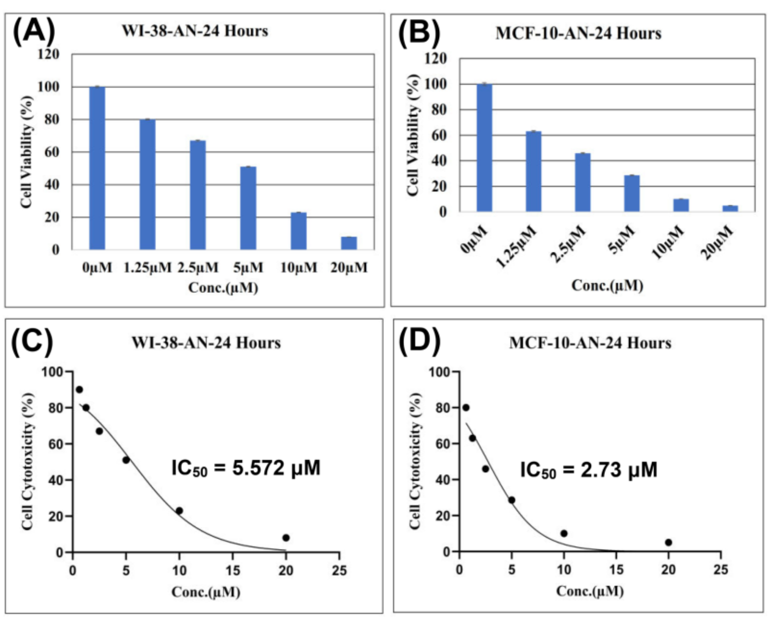

Figure S19. (A, B) The SRB assay-derived cell viability percentiles of AN in non-cancerous WI-38 and MCF-10 cell lines (n = 4) and (C, D) The SRB assay-derived cell cytotoxicity percentiles of AN in cancerous WI-38 and MCF-10 cell lines (n =4).

References

1. M. Shellaiah, T. H. Chen, T. Simon, L.-C. Li, K. W. Sun and F.-H. Ko, An Affordable Wet Chemical Route to Grow Conducting Hybrid Graphite-Diamond Nanowires: Demonstration by A Single Nanowire Device, *Sci. Rep.*, 2017, **7**, 1124; https://www.nature.com/articles/s41598-017-11741-9.
2. M. Shellaiah, N. Thirumalaivasan, K. W. Sun and S.-P. Wu, A pH cooperative strategy for enhanced colorimetric sensing of Cr(III) ions using biocompatible L-glutamic acid stabilized gold nanoparticles, *Microchem. J.*, 2021, **160**, 105754; https://www.sciencedirect.com/science/article/abs/pii/S0026265X20327673.
3. M. Shellaiah and K. W. Sun, Conjugation of cysteamine functionalized nanodiamond to gold nanoparticles for pH enhanced colorimetric detection of Cr^{3+} ions demonstrated by real water sample analysis, *Spectrochim. Acta A*, 2023, **286**, 121962; https://www.sciencedirect.com/science/article/abs/pii/S1386142522011106.
4. M. Shellaiah, B. Aazaad, M.-C. Lin, K.-W. Sun, A. Murugan, K. Anandan, M. Bhushan, M. Sivakumar and W.-T. Li, Commercial trans-β-nitrostyrene analogues for colorimetric cyanide (CN^-) detection via Michael addition-based chemodosimetric approach validated by comparative investigations, DFT, and strip method, *J. Photochem. Photobiol. A*, 2026, **472**, 116786; https://www.sciencedirect.com/science/article/abs/pii/S101060302500526X.
5. M. Shellaiah, K.-W. Sun, B. Aazaad, K. Awasthi, M.-C. Lin, N. Ohta and W.-T. Li, A perylene derivative for multi-hazard detection in environmental monitoring: Demonstration via DFT, cellular imaging, and real-time applications, *J. Hazard. Mater. Adv.*, 2025, **19**, 100863; https://www.sciencedirect.com/science/article/pii/S2772416625002748.

6. M. Shellaiah, P. Venkatesan, N. Thirumalaivasan, S.-P. Wu and K.-W. Sun, Pyrene-Based Fluorescent Probe for "Off-on-Off" Sequential Detection of Cu^{2+} and CN^{-} with HeLa Cells Imaging, *Chemosensors* 2023, **11**, 115; https://www.mdpi.com/2227-9040/11/2/115.

7. M. Shellaiah, Y.-T. Chen, N. Thirumalaivasan, B. Aazaad, K. Awasthi, K. W. Sun, S.-P. Wu, M.-C. Lin and N. Ohta, Pyrene-Based AIEE Active Nanoprobe for Zn^{2+} and Tyrosine Detection Demonstrated by DFT, Bioimaging, and Organic Thin-Film Transistor, *ACS Appl. Mater. Interfaces*, 2021, **13**, 28610-28626; https://pubs.acs.org/doi/10.1021/acsami.1c04744.